

Feasibility of Electric Power Transmission by DC Superconducting Cables

Pritindra Chowdhuri, *Fellow, IEEE*, Chandralekha Pallem, *Student Member, IEEE*, Jonathan A Demko, and Michael J Gouge

Abstract—The electrical characteristics of dc superconducting cables of two power ratings were studied: 3 GW and 500 MW. Two designs were considered for each of the two power ratings. In the first design, the SUPPLY stream of the cryogen is surrounded by the high-voltage high-temperature superconductor cylinder. The RETURN stream of the cryogen is on the grounded side of the system. In the second design, both the SUPPLY and the RETURN streams of the cryogen are on the grounded side of the cable. Two electrical characteristics of these cables were studied: 1) fault currents and 2) current harmonics. It was concluded that neither the fault currents nor the current harmonics pose any problems in the operation of the dc superconducting cables.

Index Terms—DC superconducting cable, high-temperature superconductivity, power transmission lines.

I. INTRODUCTION

INCREASING demand for electric power coupled with lack of corridors for power transmission and distribution has resulted in congestion in the power corridors with the attendant problem of instability in power delivery. Concurrently, the demand for higher power quality is increasing. Overhead power lines, being exposed to the elements of nature, are vulnerable to outages. However, overhead power lines have traditionally been built because of their cost advantages.

In spite of the cost effectiveness of the overhead power lines, the development of underground cables has been phenomenal during the entire twentieth century. The basic advantage of a superconducting cable is that it can transport the same amount of electric power as any other transport means but at lower voltage level. As the cost of power is a function of voltage as well as current, electric power transport by superconducting cable is a viable alternative. Also, the significantly higher power density in a superconducting cable than that in the other alternative power transport systems makes it an attractive means to transport cost-effective electric power over long distances. Low-temperature dc superconducting cable with supercritical helium as

cryogen was studied in Los Alamos National Laboratory in the 1970s [1].

The refrigeration system of a superconducting cable is one of the principal items of the capital cost. The introduction of the high-temperature superconductors (HTS) has increased the possibility of industrial application of superconducting cables significantly because 1) nitrogen as a cryogen, in comparison to helium, is in abundant supply and, therefore, is inexpensive, and 2) the efficiency of the higher temperature (77 K) nitrogen-cooled refrigeration system is considerably higher than the helium-cooled (10 K) refrigeration system.

Comparing ac and dc superconducting cables, the power-handling capability of an ac superconducting cable is limited by the stability limit of the power system; the dc superconducting cable has no such constraint. The charging current of an ac superconducting cable can be a significant fraction of the load current, particularly for long cables, thus reducing the power-handling capability of an ac cable considerably. Moreover, the large capacitance of a long ac superconducting cable will impose a capacitive load to the power system, causing voltage regulation problems. The system will require reactive compensation at frequent intervals along the length of the ac cable. A dc superconducting cable does not suffer from this constraint. An ac superconducting cable has hysteresis and eddy-current losses in the superconductor and its stabilizer caused by the ac magnetic flux, in addition to the dielectric losses. These “cold” temperature losses when translated to the room temperature, will demand higher refrigeration power to maintain the cable at the superconducting temperature. Moreover, the high fault-current level in the ac system may drive the superconductor to “normal” which may cause damage to the superconductor. External fault current limiters may be required in the ac superconducting cable system to prevent the conductor from going normal. In fact, no ac circuit breaker exists today which can continuously carry the full-load current required for an ac superconducting cable, let alone the interruption of fault currents. A dc superconducting cable does not need a dc circuit breaker for point-to-point power transmission. The converters at either end of the dc cable will act as electronic circuit breakers, in addition to their primary function of power conversion. Because of the fast response time of the converters, the fault currents are limited to low values, thus minimizing the hazard of the superconductor going “normal.”

Although a dc superconducting cable may be the most suitable choice for long-distance high-power transmission of electrical energy, the electrical performance of the dc superconducting cable under commercial operating conditions should be thoroughly investigated.

Manuscript received March 1, 2005; revised July 28, 2005. This paper was recommended by Associate Editor S. W. Schwenlerly. This work was supported by the State of Tennessee, Department of Economic and Community Development under Contract ED-03-01024-01, and by the Center for Electric Power, Tennessee Technological University.

P. Chowdhuri and C. Pallem are with the Center for Energy Systems Research, Tennessee Technological University, Cookeville, TN 38505 USA (e-mail: pchowdhuri@tntech.edu; cpallem21@tntech.edu).

J. A. Demko and M. J. Gouge are with the Applied Superconductivity Group, Oak Ridge National Laboratory, Oak Ridge, TN 37831 USA (e-mail: demkoja@ornl.gov; gougemj@ornl.gov).

Digital Object Identifier 10.1109/TASC.2005.859046

Unlike normal (copper or aluminum) conductors, a superconductor has no tolerance for temporary overcurrent conditions; if the current exceeds the critical current limit of the superconductor, it will go “normal” and may be severely damaged. A fault in the cable system, e.g., a flashover of an insulator at the inverter end, will cause the cable current to rise. The cable may go “normal” if the fault current exceeds the critical current of the superconductor. Therefore, one needs to estimate the magnitude and duration of the fault current.

Although there are no eddy-current and hysteresis losses in the superconducting tapes for operation in a dc system, such losses will be encountered in an actual system because of the presence of current harmonics generated by power conversion at either end of the cable. Therefore, it is essential to know the magnitude of the harmonic currents to assess the ac losses of the cable.

The magnitude and duration of fault currents and the magnitude of the harmonic currents were investigated for two possible applications in Tennessee: 1) a 100-km-long 3-GW cable in the Tennessee Valley Authority (TVA) region, and 2) a 500-m-long 500-MW cable in the Nashville Electric Service (NES) region.

II. DESIGNS OF THE CABLES

Initially, two types of dielectric design were considered: 1) cold-dielectric design, and 2) warm-dielectric design. The warm-dielectric design was rejected because of the following reasons:

- 1) Two separate cables with warm dielectric will be required to complete the electrical circuit as compared with one coaxial cable with the cold dielectric design.
- 2) The warm-dielectric design will produce magnetic fields in the area surrounding the cables. The cold-dielectric coaxial design will have no external magnetic field.
- 3) The electric strength and life expectancy of the cold dielectric will be higher than that of the warm dielectric.

The basic assumptions were the following:

- 1) Yttrium barium copper oxide (YBCO) HTS tapes will be used. The tape dimensions are: average width = 4.1 mm; average thickness = 0.3 mm; steady-state rating = 400 A/tape at 66 K. Two layers of tapes will be wound with opposite pitch angle, the pitch angle being 20°.
- 2) Wall thickness of stainless steel tubes = 1/8 in = 3.17 mm.
- 3) Cryogen flow cross-section = 2 in² = 1290.32 mm².
- 4) Thickness of thermal insulation (vacuum space) = 1 in = 25.4 mm.
- 5) Maximum steady-state electric field in dielectric, E_{\max} = 20 kV/mm.

The dielectric of a dc cable must be designed to withstand 1) the steady-state dc stress, 2) the impulse stress under transient overvoltages, and 3) the polarity reversal test. Sparse data are available for dielectrics impregnated with liquid nitrogen [2]. The data from [2] are shown in Table I for liquid nitrogen impregnated paper at 100 K.

Reference [3] published the following data on the electric strength for kraft paper impregnated with liquid nitrogen at

TABLE I
DIELECTRIC STRENGTH OF LIQUID NITROGEN IMPREGNATED PAPER AT 100 K

Type of Stress	Electric Strength (kV/mm)
DC	228.6
Impulse	175
Polarity Reversal	142.9
AC (r.m.s.)	78.6

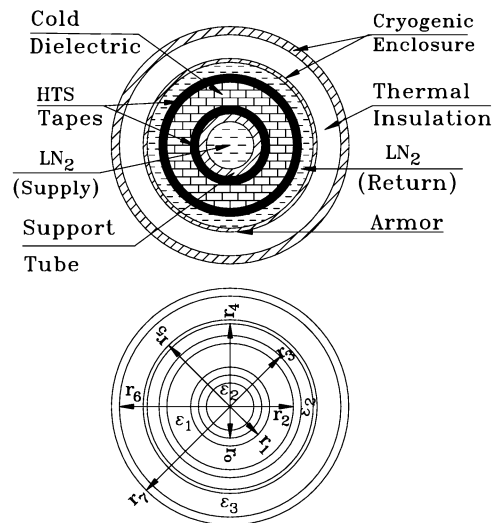


Fig. 1. Cross-sectional view of dc superconducting cable: Base design. r_o = outer radius of support tube; r_1 = inner radius of dielectric = r_o + thickness of two layers of HTS tape; r_2 = outer radius of dielectric; r_3, r_4 = inner and outer radii of RETURN LN₂ annulus; r_5, r_6 = inner and outer radii of the annulus of cryogenic envelop; r_7 = outer radius of steel pipe; ϵ_1 = permittivity of dielectric; ϵ_2 = permittivity of LN₂; ϵ_3 = permittivity of thermal insulation.

77 K: ac (root mean square) stress = 70 kV/mm, and impulse stress = 100 kV/mm. Therefore, the design value of 20 kV/mm of steady-state dc stress is a conservative number.

The cable systems were designed with two design options, each with two possible voltage ratings. The first design (base design) is based on the premise that the SUPPLY LN₂ (liquid nitrogen) flows through the central canal of the support former for the cable and the RETURN LN₂ flows in an annulus surrounding the dielectric (Fig. 1). In this design, the SUPPLY LN₂ stream is at high voltage. High-voltage bushings will be required at each refrigeration station for the cooling of the cryogen. The second design (Demko design) is based on the premise that both the SUPPLY and RETURN LN₂ streams will be on the grounded side of the dielectric (Fig. 2). This design will eliminate the high-voltage bushings at each refrigeration station for the SUPPLY LN₂ to circulate. The cryogenic systems for both design options were designed based on [4].

A. 3-GW Cables

For the 3-GW system, the $(n - 1)$ -contingency rule was applied. This contingency rule requires that 3 GW of power must be transported by multiple cables, and that if one of the cables is out of service, then the remaining cables must carry the full 3-GW load.

Three alternative designs were studied to satisfy the contingency requirement: 1) one 3-GW cable, 2) three 1.5-GW cables, and 3) four 1-GW cables. The 3-GW cable was designed for the

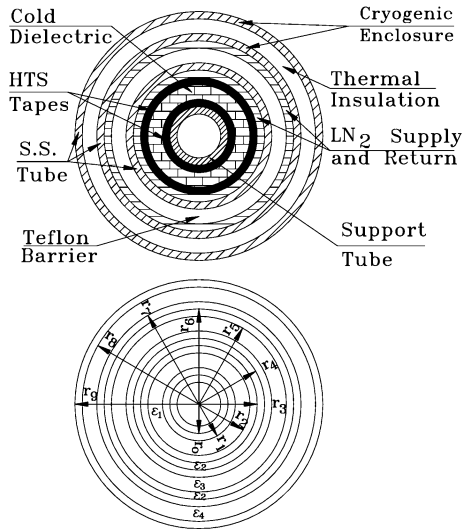


Fig. 2. Cross-sectional view of dc superconducting cable: Demko design. r_o = outer radius of support tube; r_1 = inner radius of dielectric = r_o + thickness of two layers of HTS tape; r_2 = outer radius of dielectric; r_3, r_4 = inner and outer radii of SUPPLY LN₂ annulus; r_5 = outer radius of Teflon tube 1 = inner radius of RETURN LN₂ annulus; r_6 = outer radius of RETURN LN₂ annulus; r_7 = outer radius of Teflon tube 2 = inner radius of annulus of cryogenic envelop; r_8 = outer radius of annulus of cryogenic envelop = inner radius of steel pipe; r_9 = outer radius of steel pipe; ϵ_1 = permittivity of dielectric; ϵ_2 = permittivity of LN₂; ϵ_3 = permittivity of Teflon; ϵ_4 = permittivity of thermal insulation.

purpose of reference. Of course, two 3-GW cables would have satisfied the contingency requirement. However, it may not be economically viable to design a 6-GW system to transmit only 3-GW power during normal operation. The dimensions of the cables for the base design and different contingency options are shown in Table II, and for the Demko design in Table III.

B. 500-MW Cables

The 500-MW cable is only 500 m long. Its possible application is in a tunnel underneath railroad tracks in Nashville. It has no requirement for contingency. Therefore, one 500-MW cable was designed for two possible voltage ratings for each of the base and Demko designs. The dimensions are shown in Tables IV and V.

III. ANALYSIS AND RESULTS

A. Fault Currents

The most severe fault current through the dc cable will occur if the line-end bushing of the inverter-side smoothing reactor flashes over (Fig. 3). The fault current will consist of two components. The first component will be a traveling wave caused by the discharge of the cable capacitance. The second component will be driven by the voltage source on the ac side of the rectifier.

The magnitude and duration of the cable discharge current cannot be controlled by any external means, such as valve control of the converter or a dc circuit breaker. The second component can be controlled by these external means, and the fault current profile will depend upon the characteristics of the fault

interrupter. The fault current analysis followed the techniques proposed in [5].

1) *Discharge Current of the DC Cable:* A rectangular traveling current wave I_d will be generated at the flashover point at the instant of flashover. This current wave will travel along the cable until it encounters a discontinuity at the rectifier-end smoothing reactor. Part of this current will penetrate the rectifier-end smoothing reactor and the rest will be reflected back to the cable. Because of the large impedance of the smoothing reactor relative to the surge impedance of the cable, most of the current will be reflected back to the cable, i.e., $I_r = -I_d$. This reflected current wave will travel back along the cable toward the fault location, canceling the forward current wave as it progresses. The magnitude and duration of the discharge current at the point of flashover are given by

$$I_d = \frac{V_{dc}}{Z_c} \quad (1)$$

and

$$\tau = \frac{2\ell}{v} \quad (2)$$

where I_d = discharge current, V_{dc} = dc voltage of the cable, $Z_c = \sqrt{(L)/(C)}$ = surge impedance of the cable, τ = duration of the discharge current at the flashover point, ℓ = cable length, v = velocity of propagation of the current wave in the cable, and L and C = inductance and capacitance per meter of cable. The duration of the discharge current diminishes monotonically along the cable and is zero at the rectifier end.

2) *Component of Fault Current Caused by AC-Side Voltage:* This second component of fault current will be maintained by the voltage sources on the ac side of the rectifier. Therefore, the ac-side reactances, the smoothing reactor, and the cable reactance will limit this component of the fault current.

The following assumptions were made:

- 1) Fault current is initiated at the beginning of commutation.
- 2) There is no commutation overlap.
- 3) The firing of all the valves is blocked subsequent to fault initiation.
- 4) Firing angle delay is zero.
- 5) Converters operate in 12-pulse mode.
- 6) AC network reactance beyond the rectifier transformer is negligible.

The 12-pulse system and its equivalent circuit for the computation of the fault current are shown in Fig. 4 where line-commutated thyristors have been used.

If the fault starts when the reference valve comes into conduction, the fault current will continue to increase until the ac voltage in the loop is zero, even if the sensing system is fast enough to block the next valve. The fault current will then decrease, becoming zero when $\int V_{ac} dt = 0$. If the next valve is not blocked, then the fault current will continue to rise until the new voltage around the loop is zero. Similarly, as the subsequent valves are not blocked, the fault current will continue to rise.

TABLE II
DIMENSIONS OF CABLES FOR 3-GW SYSTEM: BASE DESIGN

V_{dc} kV	No. of Tapes/Layer	r_0 mm	r_1 mm	r_2 mm	r_3 mm	r_4 mm	r_5 mm	r_6 mm	r_7 mm
<i>No Contingency: One 3-GW Monopolar Cable</i>									
200	19	23.44	24.04	36.44	37.04	42.22	45.40	70.80	73.97
300	13	23.44	24.04	44.87	45.47	49.78	52.95	78.35	81.53
<i>Single Contingency: Three 1.5-GW Monopolar Cables</i>									
100	19	23.44	24.04	29.60	30.20	36.37	39.54	64.94	68.12
150	13	23.44	24.04	32.84	33.44	39.10	42.28	67.68	70.85
<i>Single Contingency: Four 1.0-GW Monopolar Cables</i>									
75	17	23.44	24.04	28.10	28.70	35.13	38.31	63.71	66.88
100	13	23.44	24.04	29.60	30.20	36.37	39.54	64.94	68.12

TABLE III
DIMENSIONS OF CABLES FOR 3-GW SYSTEM: DEMKO DESIGN

V_{dc} kV	No. of Tapes/Layer	r_0 mm	r_1 mm	r_2 mm	r_3 mm	r_4 mm	r_5 mm	r_6 mm	r_7 mm	r_8 mm	r_9 mm
<i>No Contingency: One 3-GW Monopolar Cable</i>											
200	19	13.19	13.79	28.48	29.08	35.44	43.29	47.80	50.98	76.38	79.55
300	13	9.03	9.63	45.73	46.33	50.57	58.42	61.83	65.01	90.41	93.58
<i>Single Contingency: Three 1.5-GW Monopolar Cables</i>											
100	19	13.19	13.79	19.82	20.42	28.77	36.62	41.85	45.03	70.43	73.60
150	13	9.03	9.63	20.98	21.58	29.61	37.46	42.59	45.76	71.16	74.34
<i>Single Contingency: Four 1.0-GW Monopolar Cables</i>											
75	17	11.81	12.41	16.78	17.38	26.70	34.55	40.06	43.23	68.63	71.81
100	13	9.03	9.63	16.18	16.78	26.31	34.16	39.72	42.90	68.30	71.47

TABLE IV
DIMENSIONS OF A 500-MW MONOPOLAR CABLE: BASE DESIGN

V_{dc} kV	No. of Tapes/Layer	r_0 mm	r_1 mm	r_2 mm	r_3 mm	r_4 mm	r_5 mm	r_6 mm	r_7 mm
50	13	23.44	24.04	26.68	27.28	33.98	37.16	62.56	65.73
100	7	23.44	24.04	29.60	30.20	36.37	39.54	64.94	68.12

TABLE V
DIMENSIONS OF A 500-MW MONOPOLAR CABLE: DEMKO DESIGN

V_{dc} kV	No. of Tapes/Layer	r_0 mm	r_1 mm	r_2 mm	r_3 mm	r_4 mm	r_5 mm	r_6 mm	r_7 mm	r_8 mm	r_9 mm
50	13	9.03	9.63	12.48	13.08	24.12	31.97	37.85	41.03	66.43	69.60
100	7	4.86	5.46	13.64	14.24	24.77	32.62	38.40	41.58	66.98	70.15

The voltage across the 12-pulse rectifier bridge and the fault-current profile are shown in Fig. 5. The peak of the fault current is given by

$$i_{mn} = \frac{(n_m + 1)(A_{11} + A_{21}) + A_{12} + A_{22}}{L_{total}} \quad (3)$$

where n_m = number of misfire of the valves in the rectifier bridge, $L_{total} = L_c + L_s + L_\ell$ and the areas, A_{11} , A_{21} , A_{12} , and A_{22} are shown in Fig. 5.

The details of the analyses are given in [5], [6]. The fault current profiles for the 3-GW 200-kV base design are shown in Fig. 6. The discharge currents, the peak fault currents and their durations are tabulated in Tables VI–IX for both the 3-GW and 500-MW systems for all the design alternatives. The fault and discharge currents will be superimposed on the steady-state dc currents. These fault current magnitudes and durations are



Fig. 3. Flashover of line-end bushing of inverter-side smoothing reactor.

typically less than that of an ac cable where fault currents can reach 50 kA or more and durations can be 5–15 cycles.

B. Harmonic Currents

The source of harmonics in the dc cable are the converters at either end of the cable. The converters are considered to be the voltage sources for the dc-side harmonics. The computation of the harmonics in the 3-GW 100-km cable was based on the standing-wave theory of long transmission lines.

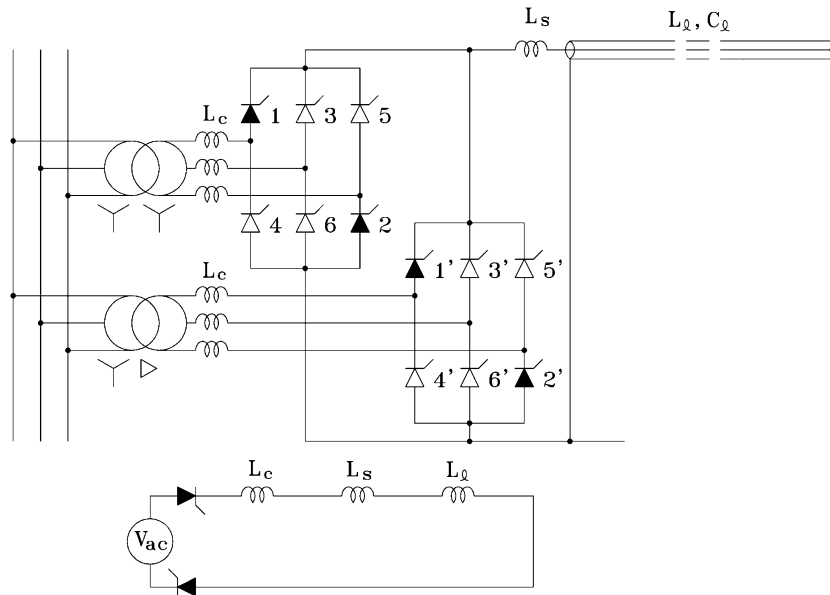


Fig. 4. Representation of a 12-pulse parallel-connected rectifier bridge with fault at inverter end. L_c = commutating inductance; L_s = smoothing inductance; L_l, C_l = inductance and capacitance of the cable.

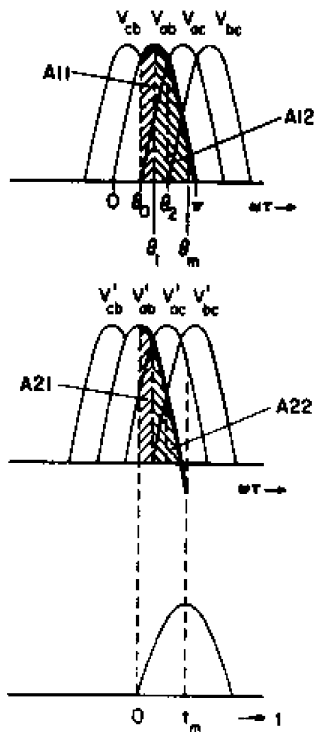


Fig. 5. Voltage across 12-pulse rectifier bridge and current profile under fault condition.

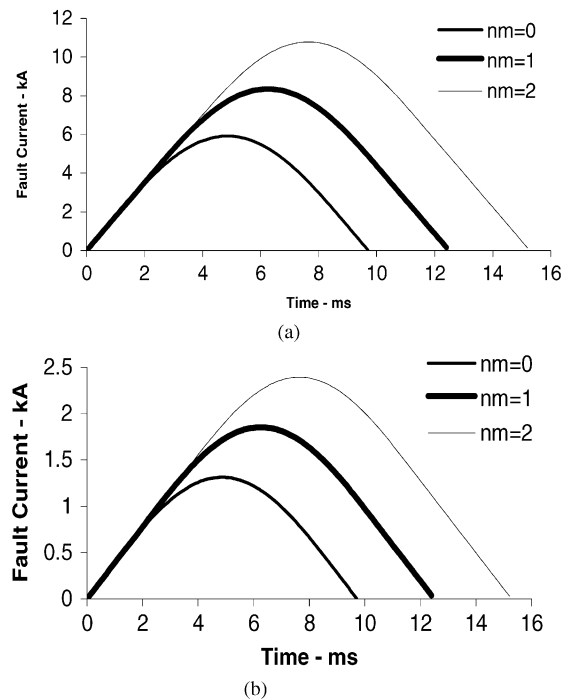


Fig. 6. Fault current profiles of the 3-GW 200-kV 100-km-long base design. Twelve-pulse converter bridge connected in parallel; commutating reactance = 0.15 p.u. (a) Smoothing reactor, L_s = 100 mH. (b) Smoothing reactor, L_s = 500 mH.

For the 500-MW 500-m cable, the cable was represented as a π -network. It was assumed that the dc cable was terminated at either end by smoothing reactors L_s . No other filter network was connected to the cable. The equivalent circuits for the long and short cables are shown in Fig. 7.

For the long cable (3-GW, 100-km), the harmonic voltages generated at either end will be attenuated by the smoothing reactors L_s and will travel along the cable in opposite directions

with almost no attenuation but changing phase. They will be reflected by the reactors repeatedly as they travel back and forth along the cable. The magnitude of a harmonic at any point along the cable will be the algebraic sum of these two components. As a result, the harmonic voltage or current level will exhibit standing wave patterns with successive maxima and minima. The maxima occur when these two components are in phase, minima when they are out of phase by π radians.

TABLE VI
 FAULT CURRENTS IN 3-GW 100-kM SYSTEM: BASE DESIGN COMMUTATING REACTANCE = 0.15 p.u.; $p_n = 12$; $n_m = 1$

Rated Voltage kV	Cable Inductance nH/m	Cable Capacitance nF/m	Smoothing Inductance mH	Discharge Current		Fault Current	
				Peak kA	Duration ms	Peak kA	Duration ms
<i>No Contingency i.e., One 3-GW Monopolar Cable</i>							
200	83.19	0.3339	100	12.67	1.054	8.352	12.5
			250			3.609	
			500			1.854	
300	124.8	0.2226	100	12.67	1.054	11.387	12.5
			250			5.188	
			500			2.72	
<i>Single Contingency i.e., Three 1.5-GW Monopolar Cables</i>							
100	41.6	0.6678	100	12.67	1.054	4.451	12.5
			250			1.854	
			500			0.939	
150	62.4	0.4452	100	12.67	1.054	6.339	12.5
			250			2.72	
			500			1.394	
<i>Single Contingency i.e., Four 1-GW Monopolar Cables</i>							
75	31.2	0.8904	100	12.67	1.054	3.386	12.5
			250			1.398	
			500			0.707	
100	41.6	0.6678	100	12.67	1.054	4.392	12.5
			250			1.843	
			500			0.937	

The details of the analysis have been discussed in [5] and [7]. The magnitudes and phase angles of the generated harmonic voltages, V_1 and V_2 , will generally be different. As the ac systems on either side of the dc system are asynchronously connected, the phase angles will vary at random. Computations were made for the cases when the two harmonic voltage sources are equal in magnitude (i.e., the ac system voltages feeding the rectifier and inverter are equal), but differ in phase angle δ by 0 and π . The equations for the harmonic currents are given by [5]

$$I_{\max} = \frac{V_n}{2\pi f_n L_s \sin(\beta\ell/2)}, \quad \text{for } \delta = 0 \quad (4a)$$

$$I_{\max} = \frac{V_n}{2\pi f_n L_s \cos(\beta\ell/2)}, \quad \text{for } \delta = \pi \quad (4b)$$

where

- V_n = generated harmonic voltage V ;
- f_n = harmonic frequency Hz ;
- L_s = inductance of smoothing reactor H ;
- β = $2\pi f_n/v$, rad/m;
- v = velocity of propagation in cable m/s ;
- ℓ = length of cable m .

The results are shown in Table X for the base design. As the magnitudes of the current harmonics are independent of the cable dimensions, for a given cable length, the magnitudes of the current harmonics for the Demko design are the same as in Table X.

The ripple losses at 720 Hz (12th harmonic) were computed for the worst case for each design, i.e., highest ripple currents and lowest smoothing inductance. The monoblock model was used [8], [9]. The monoblock model assumes that the HTS is not fully penetrated and that the ac losses are the same for this condition whether there is a dc transport current or not. In reality, the harmonic losses will even be lower when the superimposed dc transport is considered [10].

For the short cable (500-MW, 500-m), as shown in Fig. 7(b), the current, I_3 , through L_l is the harmonic current in the cable. Filter capacitances can be incorporated into the admittances, if necessary. The equation for I_3 is given by [5]

$$I_3 = \frac{V_1 - V_2}{4\pi f_n L_s \cos^2(\beta\ell/2) + Z_c \sin \beta\ell}, \quad (5)$$

where

- V_1, V_2 = generated harmonic voltages at either end of the cable V ;
- Z_c = surge impedance of the cable Ω .

Equation (5) shows that if $V_1 = V_2$, no harmonic current will exist. Therefore, computations were made for $V_1 = -V_2$. Results are shown in Table XI for the base design. The harmonic current for the Demko design will be practically the same because the term, $Z_c \sin \beta\ell$, in the denominator is negligible for the short length of cable. Because of the significantly smaller harmonic currents of the 500-MW system, the ac losses will be negligible.

TABLE VII
 FAULT CURRENTS IN 500-MW 500-M SYSTEM: BASE DESIGN COMMUTATING REACTANCE = 0.15 p.u.; $p_n = 12$; $n_m = 1$

Rated Voltage kV	Cable Inductance nH/m	Cable Capacitance nF/m	Smoothing Inductance mH	Discharge Current		Fault Current	
				Peak kA	Duration μ s	Peak kA	Duration ms
50	20.8	1.336	100	12.67	5.27	2.283	12.5
			250			0.936	
			500			0.472	
100	41.6	0.6678	100	12.67	5.27	4.057	12.5
			250			1.782	
			500			0.921	

TABLE VIII
 FAULT CURRENTS IN 3-GW 100-kM SYSTEM: DEMKO DESIGN COMMUTATING REACTANCE = 0.15 p.u.; $p_n = 12$; $n_m = 1$

Rated Voltage kV	Cable Inductance nH/m	Cable Capacitance nF/m	Smoothing Inductance mH	Discharge Current		Fault Current	
				Peak kA	Duration ms	Peak kA	Duration ms
<i>No Contingency i.e., One 3-GW Monopolar Cable</i>							
200	145	0.1915	100	7.268	1.054	7.557	12.5
			250			3.452	
			500			1.811	
300	311.5	0.0892	100	5.075	1.054	9.088	12.5
			250			4.652	
			500			2.565	
<i>Single Contingency i.e., Three 1.5-GW Monopolar Cables</i>							
100	72.52	0.3831	100	7.268	1.054	4.215	12.5
			250			1.811	
			500			0.928	
150	155.8	0.1783	100	5.075	1.054	5.556	12.5
			250			2.565	
			500			1.352	
<i>Single Contingency i.e., Four 1-GW Monopolar Cables</i>							
75	60.44	0.4596	100	6.541	1.054	3.221	12.5
			250			1.369	
			500			0.699	
100	103.8	0.2675	100	5.075	1.054	4.001	12.5
			250			1.771	
			500			0.918	

IV. DISCUSSION

A. Fault Currents

Under normal circumstances, the current controller in the rectifier station of a dc transmission system controls the load current flow to the preset value by adjusting the firing angle of the thyristors [11], [12]. This controller tries to minimize the fault current by phasing back the thyristor firing angle. However, its response is not fast enough to be of any significance under fault conditions. Therefore, the influence of the current controller was neglected in this analysis.

For a fault on the dc line of a conventional dc system, the rectifier valves are phased back to put the bridge in the inverter mode [11], [12]. The converters at both terminals then operate in the inverter mode, discharging the energy stored in the dc system to the ac system until the current becomes zero. The ac-side circuit breakers are used for backup protection.

In our analysis, the next valve to conduct (after fault initiation) is blocked by not firing its gate. The fault current con-

tinues to increase until the ac voltage in the loop becomes zero. The fault component of current will then decrease until it is zero when $\int V_{ac} dt = 0$, and the prefault load current flows. The objective of the analysis was to estimate the magnitude and the duration of the fault current above the steady-state rated current of the HTS tapes in order to decide if the HTS tapes could withstand the overload without going “normal.” Phasing back the rectifier valves into the inverter mode will lower the magnitude and duration somewhat.

The load may be restored after fault clearing by restarting the converters by ramping up the direct voltage and current [11], [12].

The assumption of firing delay angle, $\alpha = 0$, in this study will result in the maximum fault component of current. Usually α is greater than zero. In that case, the fault component of current will be less.

Higher dc system voltage will increase the discharge current. However, higher system voltage requires thicker insulation between the two coaxial HTS cylinders. Thicker insulation

TABLE IX
 FAULT CURRENTS IN 500-MW 500-M SYSTEM: DEMKO DESIGN COMMUTATING REACTANCE = 0.15 p.u.; $p_n = 12$; $n_m = 1$

Rated Voltage kV	Cable Inductance nH/m	Cable Capacitance nF/m	Smoothing Inductance mH	Discharge Current		Fault Current	
				Peak kA	Duration μ s	Peak kA	Duration ms
50	51.92	0.535	100	5.08	5.27	2.282	12.5
			250			0.936	
			500			0.472	
100	103.8	0.268	100	5.08	5.27	4.056	12.5
			250			1.781	
			500			0.921	

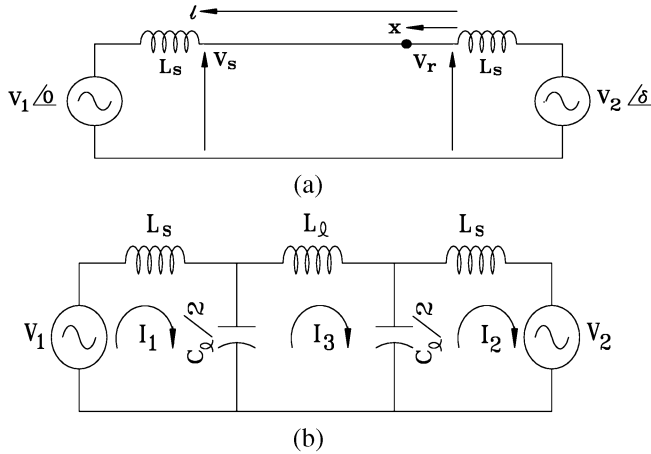


Fig. 7. Schematic representations of the dc cable system for harmonic analysis. (a) 3-GW 100-km cables; (b) 500-MW 500-m cables. V_1, V_2 = harmonic voltage sources; L_s = smoothing reactors; L_l, C_l = total inductance and capacitance of cable.

increases the inductance and decreases the capacitance of the cable, thus increasing the surge impedance of the cable. This will tend to decrease the discharge current, as shown in (1). In some designs, the discharge current may even decrease for higher system voltage as evident in Tables VI–IX. Similarly, as the fault current is driven by the ac system voltage, the fault current should be higher for higher system voltage. The discharge current is not affected by the terminal (smoothing) inductance because it is confined within the cable; it depends upon the dc voltage and the cable surge impedance. However, the fault current is significantly affected by the terminal inductance because the fault current flows from the ac-side voltage to the point of fault via the commutating inductance of the converter transformer, the terminal inductance and the cable inductance. One misfire ($n_m = 1$) of the converter valves was considered to be sufficient delay for the protection system to respond in turning the valves off.

Only one length for each of the two systems was considered, i.e., 100 km for the 3-GW system and 500 m for the 500-MW system. The duration of the discharge current is directly proportional to the cable length. The magnitude of the discharge current is independent of the length. However, the peak of the fault current will be reduced for longer length because the increased cable inductance will provide higher impedance to the flow of the fault current. As the terminal inductance is significantly higher than the cable inductance, the effect of the cable length on the fault current will not be significant.

Neither the durations nor the magnitudes of the discharge currents and the fault currents are high enough to damage the superconducting cables which would be wound with HTS tapes stabilized with a normal conductor such as copper or brass [13], [14].

B. Harmonic Currents

It should be observed in Tables X and XI that lower dc voltages of the cable produce lower harmonic currents. Lower dc voltage means lower ac-side voltage. As these ac voltages are the sources of harmonics (both voltage and current), lower dc rated voltage of the cable will produce lower harmonic current. It should also be noticed in these tables that higher smoothing inductances at the converter terminals lower the harmonic current for the same dc voltage. This is caused by higher voltage drop across the higher smoothing inductances.

The level of ac losses due to harmonic currents in the dc cables do not pose any problem for the reliable operation of the dc cables [15]. The ac losses due to the harmonic currents (Table X) are much less than the thermal heat in-leak to the cryostat which is on the order of 3–5 W/m. This means that dc harmonic filters will not be required. It will lower the cost of the converters a little and also increase the reliability of operation by eliminating some accessories in the system.

C. Comparison Between Base Design and Demko Design

The base design (Fig. 1) is the standard design where the SUPPLY stream of the cryogen flows through the core of the cable assembly and the RETURN stream envelops the second concentric HTS cylinder. This is very desirable for cryogenic considerations because of its ability to cool the cable system uniformly. The SUPPLY stream of cryogen is enclosed inside the high-voltage HTS cylinder. This SUPPLY stream of cryogen has to be taken out of the cable system at every refrigeration station for recirculation and cooling. This means that the SUPPLY stream has to penetrate through the high-voltage envelope to be delivered to the refrigeration system which is at ground potential. This can be done by designing a high-voltage bushing to be placed at each station of the refrigeration system. It will be expensive and a potential source of unreliability due to thermal, mechanical, and electric stresses. In contrast, both the cryogen streams are at ground potential under steady-state operation in the Demko design (Fig. 2). From an electrical standpoint, this design will be simpler, cost effective, and more reliable.

The discharge current during fault of the Demko design (Tables VIII and IX) is smaller than that of the base design

TABLE X
CURRENT HARMONICS IN 3-GW 100-KM SYSTEM: BASE DESIGN FIRING ANGLE, $\alpha = 15^\circ$; OVERLAP ANGLE, $u = 32.55^\circ$ COMMUTATING REACTANCE, $X_c = 0.15$ p.u.; HARMONIC NUMBER, $p_n = 12$

DC Voltage	Current	Smoothing	Harmonic Current, A @		Ripple
		Inductance			Losses
kV	kA	mH	$\delta=0$	$\delta=180^\circ$	@ 66 K
<i>No Contingency i.e. One 3-GW Monopolar Cable</i>					
		100	34.47	86.64	0.4944
200	15	250	13.79	34.66	
		500	6.89	17.33	
300	10	100	51.7	129.96	3.4615
		250	20.68	51.98	
		500	10.34	25.99	
<i>Single Contingency i.e. Three 1.5-GW Monopolar Cables</i>					
		100	17.23	43.32	0.0618
100	15	250	6.89	17.33	
		500	3.45	8.66	
150	10	100	25.85	64.98	0.4325
		250	10.34	25.99	
		500	5.17	13	
<i>Single Contingency i.e. Four 1-GW Monopolar Cables</i>					
		100	12.93	32.49	0.0323
75	13.33	250	5.17	13	
		500	2.59	6.5	
100	10	100	17.23	43.32	0.1281
		250	6.89	17.33	
		500	3.45	8.66	

TABLE XI
CURRENT HARMONICS IN 500-MW 500-M SYSTEM: BASE DESIGN FIRING ANGLE, $\alpha = 15^\circ$; OVERLAP ANGLE, $u = 32.55^\circ$ COMMUTATING REACTANCE, $X_c = 0.15$ p.u.; HARMONIC NUMBER, $p_n = 12$

DC Voltage	Current	Smoothing Inductance	Harmonic Current
kV	kA	mH	A
50	10	100	8.01
		250	3.2
		500	1.6
100	5	100	16.01
		250	6.4
		500	3.2

(Tables VI and VII) because of the higher surge impedance of the Demko design, as shown in (1). The fault component of the current for the Demko design is also somewhat lower than that for the base design because of the higher inductance of the Demko design, as shown in (3).

The harmonic currents for the base and the Demko designs were found to be the same for both the 100-km and 500-m cables. For the long cables, as shown in (4), the harmonic current is a function of the smoothing inductance L_s and the propagation constant β for given harmonic voltage V_n and harmonic frequency f_n . β is a function of the permittivity of the cable dielectric. Therefore, for the same cable length, terminal inductance, and the dielectric, the harmonic currents for the two designs must be the same. For short cables, as (5) shows, the harmonic current is a function of the surge impedance of the cable.

However, the term $\sin \beta l$ is very small, and therefore, does not affect the magnitude of the harmonic currents.

V. CONCLUSION

Neither fault current nor current harmonics will impact the steady-state operation or degrade the performance of the dc superconducting cable.

The Demko design with both GO and RETURN flows of the cryogen on the grounded side of the cable system will enhance the reliability as well as the cost effectiveness of the cable system. Further study is needed to optimize this design.

REFERENCES

- [1] P. Chowdhuri and F. J. Edeskuty, "Bulk power transmission by superconducting DC cable," *Electric Power Syst. Res.*, vol. 1, no. 1, pp. 41–49, 1977.
 - [2] A. A. Hassam-Eldin and B. Salvage, "A liquid-nitrogen-cooled, high-voltage, direct-current cable," in *Proc. Int. Conf. High Voltage DC and/or AC Power Transmission*, U.K., Nov. 19–23, 1973, IEE Conf. Publication 107.
 - [3] H. Suzuki *et al.*, "Electrical insulation characteristics of cold dielectric high temperature superconducting cable," *IEEE Trans. Dielectr. Electr. Insul.*, vol. 9, no. 6, pp. 952–963, Dec. 2002.
 - [4] J. A. Demko *et al.*, "Cryostat vacuum thermal considerations for HTS power transmission cable systems," *IEEE Trans. Appl. Supercond.*, vol. 13, no. 2, pp. 1930–1933, Jun. 2003.
 - [5] P. Chowdhuri and H. L. Laquer, "Some electrical characteristics of a dc superconducting cable," *IEEE Trans. Power App. Syst.*, vol. PAS-97, no. 2, pp. 99–408, Mar./Apr. 1978.
 - [6] H. A. Peterson, A. G. Phadke, and D. K. Reitan, "Transients in EHVDC power systems: Part I—Rectifier fault currents," *IEEE Trans. Power App. Syst.*, vol. PAS-88, no. 7, pp. 981–989, Jul. 1969.
 - [7] D. H. Welle, A. G. Phadke, and D. K. Reitan, "Evaluation of harmonic levels on an HVDC transmission line," in *Proc. American Power Conf.*, vol. 29, 1967, pp. 1100–1108.
 - [8] J. J. Rabbers, *AC loss in Superconducting Tapes and Coils*. Enschede, The Netherlands: Proefschrift Universitaet Twente, 2001.
 - [9] V. Minervini, "Two-dimensional analysis of AC loss in superconductors carrying transport current," *Adv. Cryogenic Eng. Mater.*, vol. 28, pp. 587–599, 1982.
 - [10] B. des Ligneris *et al.*, "Decrease of AC losses in high TC superconducting tapes by application of a DC current," *Adv. Cryogenic Eng. Mater.*, vol. 46, pp. 831–837, 2000.
 - [11] J. Arrillaga, *High Voltage Direct Current Transmission*. London, U.K.: Peter Perrgrinus Ltd., 1983.
 - [12] K. R. Padiyar, *HVDC Power Transmission Systems*. New York: Wiley, 1990.
 - [13] J. W. Lue *et al.*, "Fault current tests of a 5-m HTS cable," *IEEE Trans. Appl. Supercond.*, vol. 11, no. 1, pp. 1785–1788, Mar. 2001.
 - [14] J. W. Lue, M. J. Gouge, and R. C. Duckworth, "Over-current testing of HTS tapes," *IEEE Trans. Appl. Supercond.*, pt. 2, vol. 15, no. 2, pp. 1835–1838, Jun. 2005.
 - [15] J. A. Demko *et al.*, "Practical AC losses and thermal considerations for HTS power transmission cable systems," *IEEE Trans. Appl. Supercond.*, vol. 11, no. 1, pp. 1789–1792, Mar. 2001.
- Pritindra Chowdhuri** (M'52–SM'60–F'96) received the B.Sc. degree in physics and the M.Sc. degree in applied physics from Calcutta University, India, the M.S. degree in electrical engineering from Illinois Institute of Technology, Chicago, IL, and the D.Eng. degree in engineering science from Rensselaer Polytechnic Institute, Troy, NY.
- He has worked with Westinghouse Electric Corp., East Pittsburgh, Maschinenfabrik Oerlikon, Zurich, Switzerland, Forschungskommission des SEV and VSE fuer Hochspannungsfragen, Daeniken, Switzerland, General Electric Co., Pittsfield, MA, Schenectady, NY, Erie, PA, and Los Alamos National Laboratory, Los Alamos, NM. He joined the Center for Electric Power, Tennessee Technological University as a Professor of Electrical Engineering in 1986.
- He is a Fellow of the Institution of Electrical Engineers (U.K.), the American Association for the Advancement of Science, and the New York Academy of Science. He is a Member of the Power Engineering Society, Industry Applications Society, Electromagnetic Compatibility Society, and the Dielectrics and Electrical Insulation Society of the IEEE. He is also a Member of CIGRE, Paris, France. He is a registered professional engineer in Massachusetts.
- Chandralekha Pallem** (S'02) received the B.Eng. degree in electrical engineering from Jawaharlal Nehru Technological University, India, and the M.S. degree in electrical engineering from Tennessee Technological University, Cookeville, TN. She is working toward the Ph.D. degree at Tennessee Technological University.
- Her primary areas of interest are electric power systems and high voltage engineering.
- Jonathan A. Demko** received the B.S., M.S., and Ph.D. degrees in mechanical engineering from Texas A&M University.
- He has over 18 years of experience in the thermal-fluids and thermal management areas. He worked for General Dynamics/Fort Worth (currently Lockheed Martin Tactical Aircraft Systems) as the Thermodynamics Analysis Group Lead Engineer and Thermal Management Team Leader for the National Aerospace Plane (NASP) program. He also held engineering positions with the Superconducting Super Collider Laboratory Cryogenics Department. He was a Senior Member of the Technical Staff at Sandia National Laboratory. At present, he is with Oak Ridge National Laboratory where he is involved with the development of electric power applications (power cables and transformers) of high-temperature superconductors.
- He is a Member of the American Society of Mechanical Engineers (ASME) and the Cryogenic Society of America (CSA). He is a registered professional engineer in Texas.
- Michael J. Gouge** received the B.S. degree in physics with honors from the United States Naval Academy, the Ph.D. degree in physics from University of Tennessee, Knoxville, TN.
- He has been at Oak Ridge National Laboratory, Oak Ridge, TN, since 1986 working on energy programs involving cryogenic and superconducting technology. He is now leader of the Applied Superconductivity Group at Oak Ridge National Laboratory. His group presently is involved with high-temperature superconducting (HTS) cables, transformers, and generators as well as quench and stability, ac-loss, and other studies of HTS conductors and coils. Included in this R&D program is optimization of cryogenic cooling systems for these emerging technologies.